Strain Transfer of Sheet-Bonded FRP to Concrete and Masonry

Young-Joo Lee [1], Thomas E. Boothby [1], and Charles E. Bakis[2]

[1] *Department of Architectural Engineering, 104 Engineering Unit A, The Pennsylvania State University, University Park, PA 16802, USA*
[2] *Department of Engineering Science & Mechanics, 227 Hammond Bldg., The Pennsylvania State University, University Park, PA 16802, USA*

SUMMARY: Reinforced concrete tensile specimens reinforced with FRP sheets were tested during this investigation. Each of the rectangular concrete prisms was treated with a different reinforcement system. High strength carbon FRP sheet reinforcement on concrete specimens were investigated, as well as push-apart specimens of bricks. The brick specimens were reinforced with the same types of FRP, with three different sheet widths and two different bond lengths. Finite element modeling is used to predict the behavior of the specimens in the region of the sheet bonded reinforcement. Both the experimental and the analytical results show the development of high tensile strains in the concrete and in the masonry. The concrete specimens develop diagonal tensile stresses in the vicinity of transverse cracks. Masonry specimens with narrow sheet reinforcement fail by rupture of the FRP sheet. On the other hand, the masonry specimens reinforced with wider width shows an assortment of premature failure modes such as FRP sheet breakage, debonding, and brick failure. Diagonal tension cracks both along the boundary of the reinforcement and near the point where the reinforcement crosses a brick bed joint were observed. In both materials, diagonal cracks develop at locations away from the end of the reinforcing sheet. These diagonal cracks precipitate a softening and weakening of the concrete specimens and the failure of the brick specimens.

KEYWORDS: concrete, civil applications, FRP sheet, shear

INTRODUCTION

Recently, FRP sheets have been widely used in the strengthening and repair of reinforced concrete, prestressed concrete, and in unreinforced masonry structures subjected to either in-plane or out-of-plane loading [1][2]. The results show considerable strengthening, however, a variety of premature failure modes have been discovered and these must be understood and controlled [3]. Some of these failure modes result from the adhesion of the relatively compliant and high-strength reinforcement to the stiff and brittle substrate [4]. The present investigation is concerned with the strain transfer between the repair material and the substrate, and the stresses that are developed within the substrate because of the tensile resistance of the repair material.

EXPERIMENTAL PROCEDURES

Three concrete and seventeen masonry specimens reinforced with high strength CFRP sheet were investigated. The configurations of the specimens are presented in Figure 1. CFRP sheets were attached to both the precracked concrete and masonry push-apart specimens, and they were tested in tension. Three different thickness of adhesive interlayer between concrete and FRP sheet were tested for the concrete specimen. Two different types of brick with various FRP bond lengths and widths in the masonry push-apart specimen were investigated.

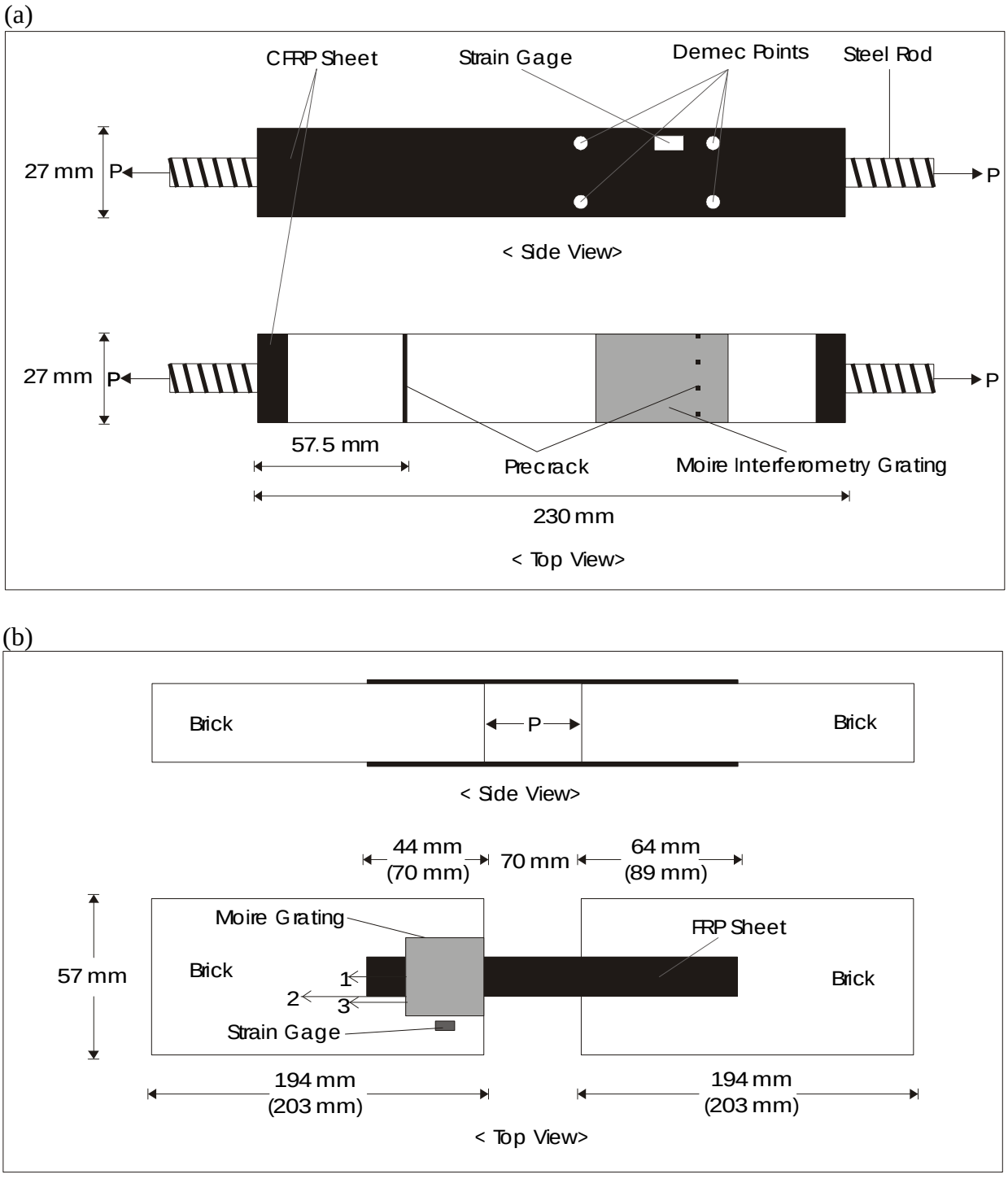

Figure 1. Configurations of Specimens:
(a) Concrete Specimen and (b) Masonry Specimen

Moiré interferometry [5] was used to measure full-field local displacement in the vicinity of the induced cracks of the concrete specimen, and along the edge of the FRP sheet in the push-apart specimen. All of the three concrete specimens and one of the masonry specimens with 25 mm sheet width were tested using moiré interferometry. A moiré diffraction grating was attached above the precrack allowing the investigation at the concrete/FRP sheet interface. It was also attached on the FRP sheet and brick near the end of the brick for the masonry push-apart specimen.

A push-apart test was performed on brick specimens in order to investigate the failure mode corresponding to the various FRP sheet bond lengths and widths as well as the different types of brick. One specimen consists of two bricks and one strip of FRP sheet with width of 13, 25, or 51 mm. The bond length on each brick is not symmetric so that the failure is expected to occur within the brick with shorter bond length. The bond length on the shorter side is considered for two cases: 44 and 70 mm (Refer to Figure 1 and Table 1 for specimen number and its detailed configuration).

In addition, finite element modeling was used to predict the behavior of the specimens in the region of the FRP sheet bonded and along the edges. The modeling for both concrete and masonry push-apart specimen was established and analyzed in linearly elastic region. For the FEM analysis, ANSYS version 5.4 was used [6].

RESULTS

Failure Mode of Masonry Specimens

Table 1 shows the results of tests performed on masonry push-apart specimen. The specimens with 13 and 25 mm sheet widths were always failed in the middle of the FRP sheet regardless of the bond length at a load consistent with the CFRP sheet tensile strength. On the other hand, the specimen with 51 mm sheet width shows various type of failure such as FRP breakage, FRP sheet debonding, and brick failure in shear. Usually, the failure mode was a combination of two different types of failure in this configuration. Figure 2 shows the representative failure modes for the specimens with different sheet width.

Moiré Interferometry on Concrete and Masonry Specimens

Figure 3 shows representative results of the moiré interferometry. Figure 3 (a) shows the fringes of the concrete specimen at 2.7 kN and (b) represents the fringes of push-apart specimen with 25 mm sheet width at 2.7 kN. The strain is obtained by differentiation of the displacement and then plotted using seventh order of polynomial. In the concrete specimen, the diagonal crack occurs near the precrack and a relatively large displacement occurs at the concrete/FRP sheet interface. In the masonry specimen, the strain is very concentrated at the end of the brick on the FRP sheet. Figure 4 and 5 show the result of the moiré fringe analysis for the concrete and masonry specimen, respectively. In Figure 4, the strain at 2.7kN of load level increases towards the precrack. Figure 5 shows the strain distribution along the longitudinal direction at three locations (Refer to line numbers in Figure 1). It shows the development of high strain concentrations towards the end of the brick along the edge of the FRP sheet, and the strain developed on the brick is very low.

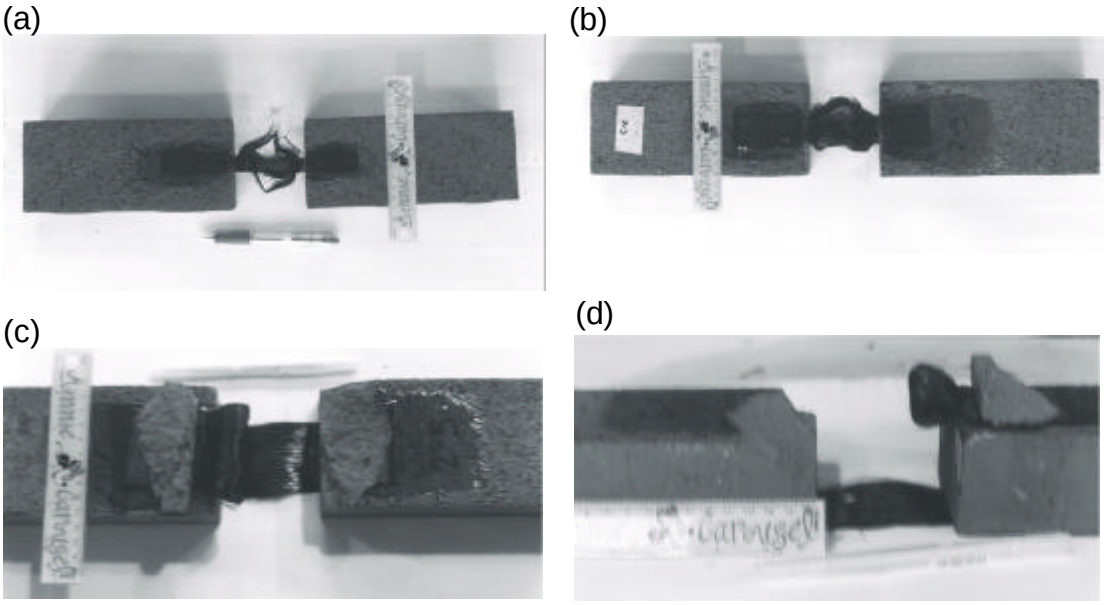

Figure 2. Failure Modes of Masonry Specimen:
(a) Specimen 2-1, 13 mm Width, (b) Specimen 2-3, 25 mm Width
(c) Specimen 2-5, 51 mm Width, (c) Specimen 2-5, Side View

Table 1. Failure Load Level and Mode

Spec. No.	Sheet Width	Bond Length	Brick Type	Failure Load	Failure Mode
1-1	13 mm	40 mm	Extruded	4.6 kN	FRP
2-1	13 mm	40 mm	Extruded	5.6 kN	FRP
3-1	13 mm	40 mm	Molded	4.7 kN	FRP
1-2	13 mm	77 mm	Extruded	6.6 kN	FRP
2-2	13 mm	77 mm	Extruded	6.4 kN	FRP
3-2	13 mm	77 mm	Molded	4.7 kN	FRP
2-3	25 mm	40 mm	Extruded	10.7 kN	FRP
3-3	25 mm	40 mm	Molded	6.3 kN	FRP
1-4	25 mm	77 mm	Extruded	12.0 kN	FRP
2-4	25 mm	77 mm	Extruded	10.7 kN	FRP
3-4	25 mm	77 mm	Molded	7.6 kN	FRP
1-5	51 mm	40 mm	Extruded	31.5 kN	FRP & Brick
2-5	51 mm	40 mm	Extruded	21.1 kN	Brick
4-5	51 mm	40 mm	Molded	18.1 kN	FRP & Debonding
6-5	51 mm	40 mm	Extruded	18.8 kN	FRP & Debonding
1-6	51 mm	77 mm	Extruded	30.9 kN	Debonding & Brick
2-6	51 mm	77 mm	Extruded	19.3 kN	FRP (severe bending)

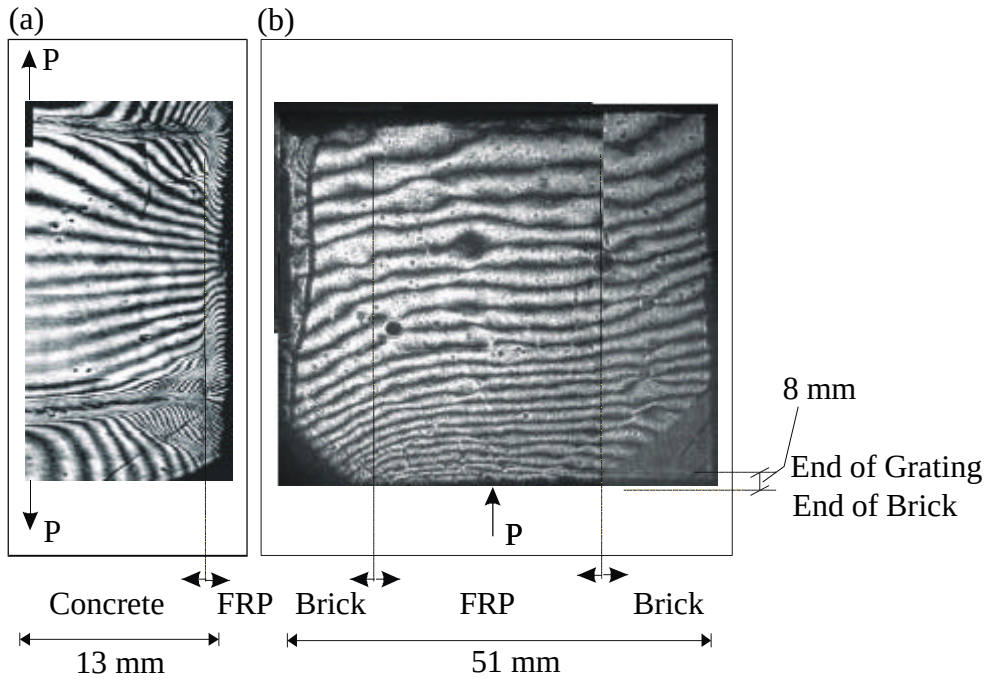

Figure 3. Moiré Fringe Images: (a) in Concrete Specimen at 2.7 kN of Load and (b) in Masonry Specimen at 5.8 kN of Load

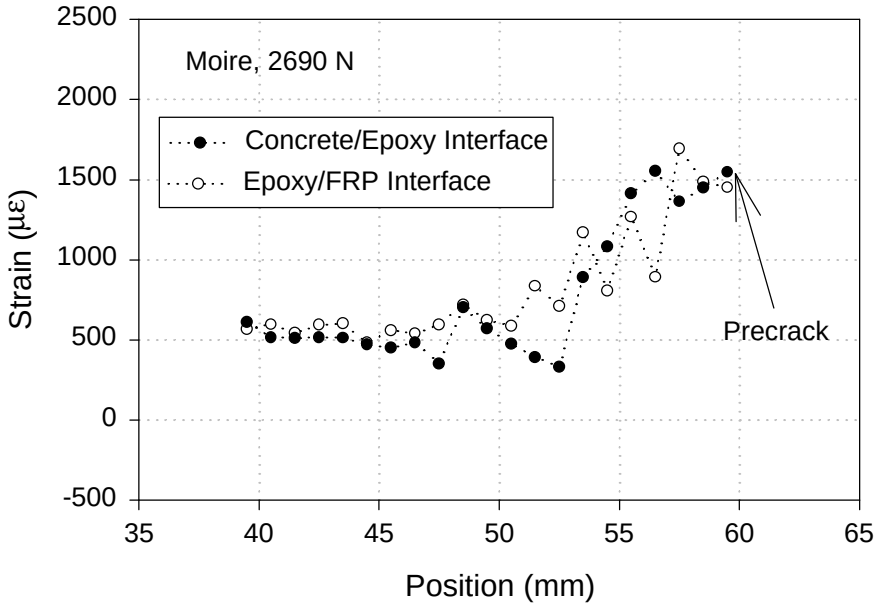

Figure 4. Strain Distribution in Concrete Specimen at 2.7 kN by Moiré Analysis

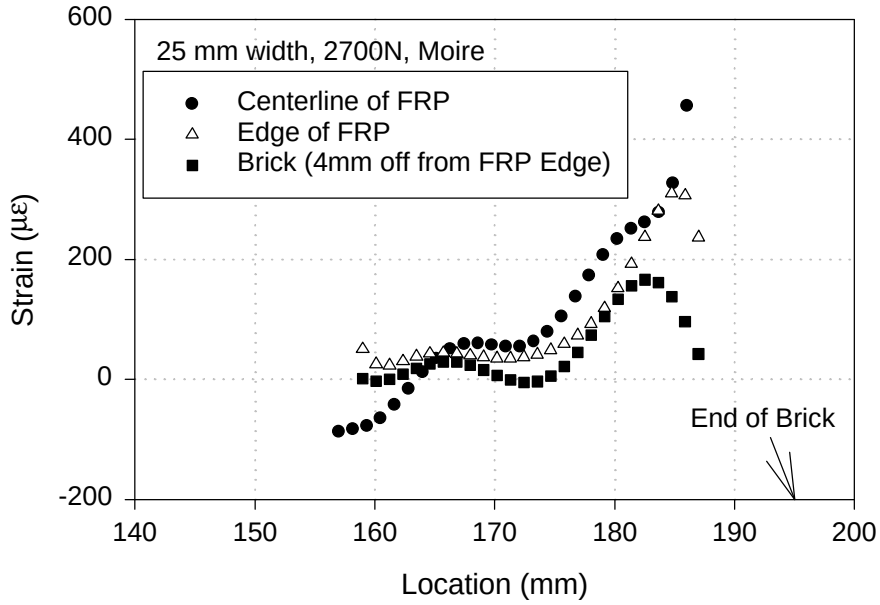

Figure 5. Strain Distribution in Masonry Specimen at 2.7 kN by Moiré Analysis

FEM Analysis on Concrete and Masonry Specimens

Finite element modeling is used to predict the behavior of the specimens in the region of the sheet bonded reinforcement. Figure 6 shows the distribution of strains at the concrete/FRP sheet interface when the primer coat thickness is assumed to be 0.2 mm. It is assumed that the specimen has already cracked between two precracks at 2.7 kN in the concrete specimen. That is, the secondary tension crack is intentionally developed between the precracks in the finite element model. As shown in the Figure, the strain is highly concentrated within 6 mm of the crack. The character and magnitude of the strains are comparable to the results of the moiré analysis shown in Figure 4.

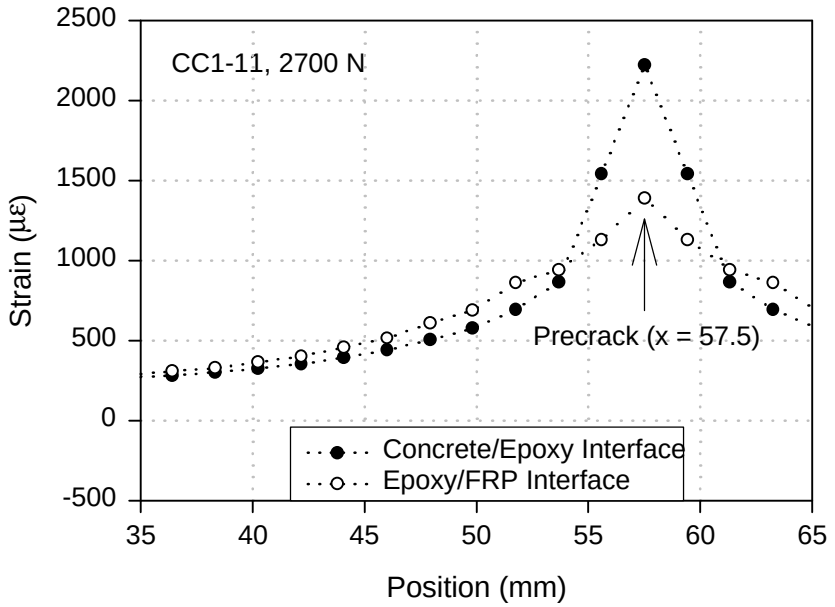

Figure 6. Strain Distribution in Concrete Specimen at 2.7 kN by FEM

Figure 7 shows the strain distribution in masonry specimen with 25 mm sheet width at 2.7 kN by FEM. The strains in the FRP sheet tends to have maximum strain at the end of the brick, while almost no strains are developed on the brick at this load level.

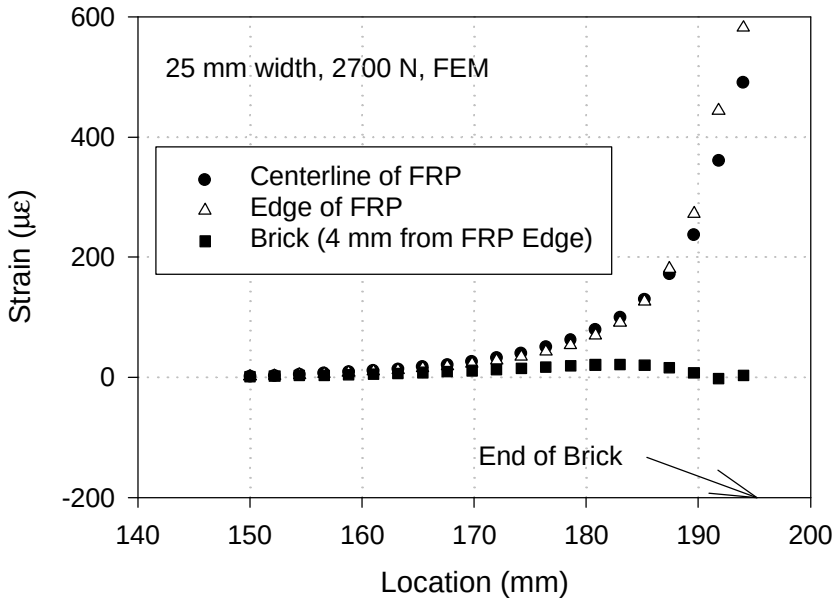

Figure 7. Strain Distribution in Masonry Specimen at 2.7 kN by FEM

Figure 8 shows the distribution of strains along the centerline and at the edge of the FRP sheet for a masonry specimen with 40 mm of bond length. The load level was chosen based on the experimental result of the molded brick specimen with short bond length. The failure of the specimens with 13 and 25 mm due to FRP rupture corresponds to the FEM result. The strain is highly large at the end of brick on the FRP sheet, while almost no strain is developed on the brick (4 mm off from the edge of the FRP sheet). It is also noted that the strain developed in the FRP sheet shows constant magnitude across the sheet width.

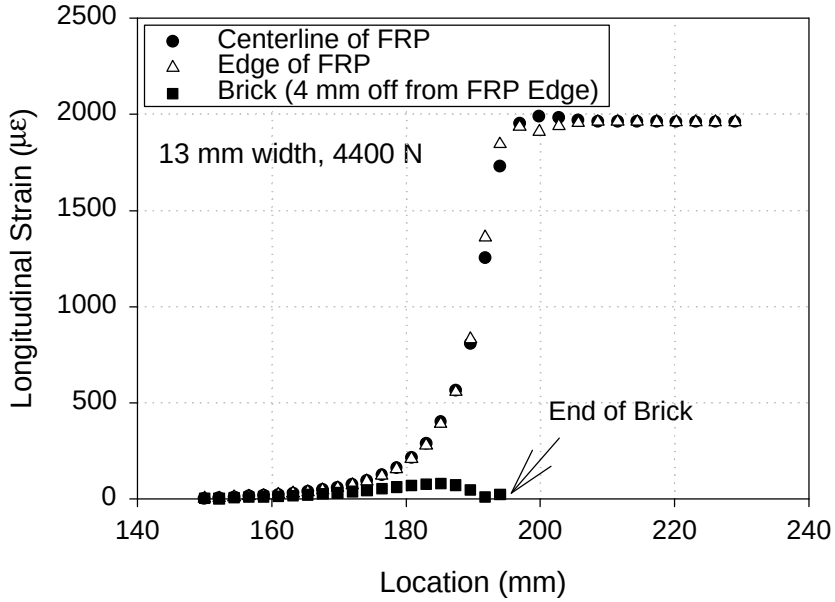

Figure 8. Strain Distribution in Masonry Specimen with 13 mm Sheet Width by FEM

For a specimen with a sheet width of 51 mm, 4 times wider, the strains are non-uniform across the width at a proportional load level, and the strains in the brick are much greater. As shown in the circled part of Figure 9, the strain is highly concentrated at the end of the brick on the FRP. The CFRP sheet used in this experiment has 1.5 % ultimate strains according to the data provided by the manufacturers [7]. It is also noticed that the strain is much greater at the edge than at the centerline of the FRP sheet where the brick ends. The shear strain developed in this region is investigated as shown in Figure 10. The shear strain is large within 6 mm of the brick along the FRP sheet edge and consistent with failure in brick, which can be expected to fail at shear strains of about 200 με. The ultimate shear strain of the epoxy is the 4.3 % [8], the specimen with 51 mm sheet width has the failure possibility of the brick in shear and debonding of the FRP sheet, which is investigated in the experiment above.

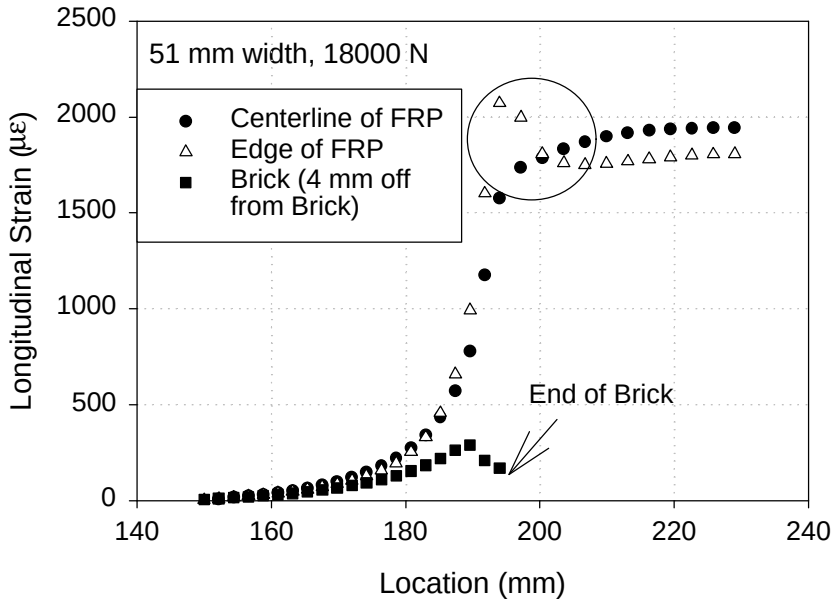

Figure 9. Strain Distribution in Masonry Specimen with 51 mm sheet width by FEM

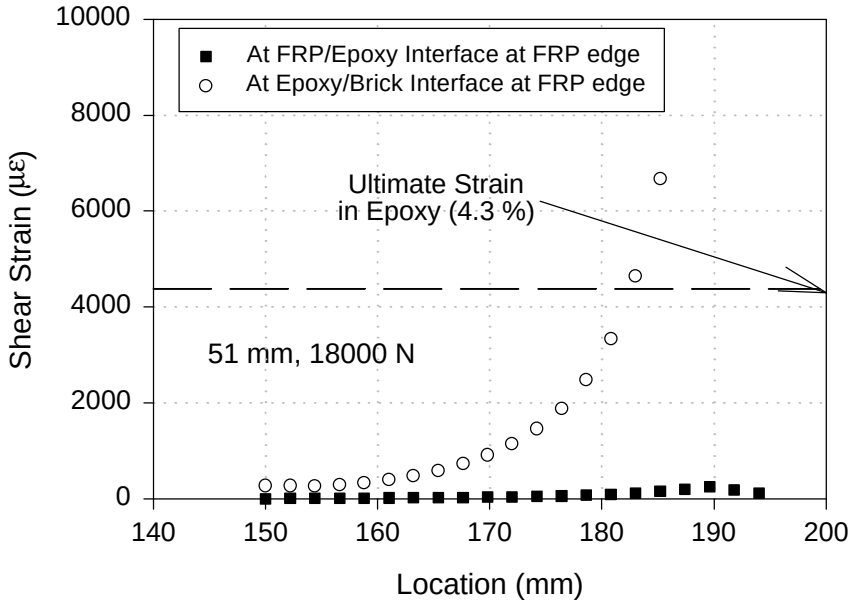

Figure 10. Shear Strain Distribution along the edge of the FRP sheet

CONCLUSIONS

As shown in the moiré result, diagonal cracks develop in the concrete specimens near the precrack. The analysis based on the finite element modeling is capable of predicting the effects of transfer of tensile stresses in FRP to brittle substrates for both concrete and masonry specimens. The brick push-apart specimen shows the failure in the FRP sheet when the epoxy is kept below of ultimate strain such as in case of the specimens with 13 and 25 mm sheet width. As width of the FRP sheet increases, the strain becomes concentrated along the edge of the FRP sheet at the end of brick as well as the strain increases in the middle of the FRP sheet. This appears to cause various failure modes such as FRP sheet breakage or debonding and brick failure in shear.

ACKNOWLEDGMENT

The authors gratefully acknowledge the financial support of the National Science Foundation under grants No. CMS - 9506736 and CMS – 9624614, and the contribution of materials by Master Builders and the Glen-Gery Corporation.

REFERENCES

1. Christensen, J. B., Gilstrap, J., Dolan, C. W., "Composite Materials Reinforcement of Existing Masonry Walls," *Journal of Architectural Engineering*, Vol. 2, No. 2, pp. 63-70, June, 1996.

2. Dolan, B. E. Hamilton, H. R. III, and Dolan, C. W., "Strengthening with Bonded FRP Laminate, " *Concrete International*, Vol. 20, No. 6, pp.51-55, June 1998.

3. Nanni, A., Bakis, C. E., and Boothby, T. E., "Externally Bonded FRP Composites for Repair of RC Structures," *Non-Metallic (FRP) Reinforcement for Concrete Structures, Proceedings of the 3rd International Symposium*, Vol.1, Oct. pp. 303-310, 1997.

4. Lee, Y. J., Tripi, J. M., Boothby, T. E., Bakis, C. E., and Nanni, A., "Tension Stiffening Model for FRP Sheets Bonded to Concrete," *2nd International Conference on Composites in Infrastructure*, Vol. 1, pp. 175-186, 1998.

5. Dally, J. W. and Riley, W. F., "Experimental Stress Analysis," *3rd Edition, McGraw-Hill, Inc*., 639p, 1991.

6. ANSYS, Inc., "Software Product and Program Documentation," Copyright, 1997, SAS IP, Inc., ANSYS 5.4.

7. Tonen Corporation, "Forca Tow Sheet Technical Notes," 1997.

8. Frigo, E. M. "The Mechanics of Externally Bonded FRP for the Repair of Reinforced Concrete," MS Thesis, The Pennsylvania State University, 199 p, 1996.